



HAL
open science

One-pot cascade syntheses of microporous and mesoporous pyrazine-linked covalent organic frameworks as Lewis-acid catalysts

Yunchao Ma, Xiaozhou Liu, Xinyu Guan, Hui Li, Yusran Yusran, Ming Xue, Qianrong Fang, Yushan Yan, Shilun Qiu, Valentin Valtchev

► To cite this version:

Yunchao Ma, Xiaozhou Liu, Xinyu Guan, Hui Li, Yusran Yusran, et al.. One-pot cascade syntheses of microporous and mesoporous pyrazine-linked covalent organic frameworks as Lewis-acid catalysts. Dalton Transactions, 2019, 48 (21), pp.7352-7357. 10.1039/C8DT05056B . hal-03039940

HAL Id: hal-03039940

<https://normandie-univ.hal.science/hal-03039940>

Submitted on 9 Dec 2020

HAL is a multi-disciplinary open access archive for the deposit and dissemination of scientific research documents, whether they are published or not. The documents may come from teaching and research institutions in France or abroad, or from public or private research centers.

L'archive ouverte pluridisciplinaire **HAL**, est destinée au dépôt et à la diffusion de documents scientifiques de niveau recherche, publiés ou non, émanant des établissements d'enseignement et de recherche français ou étrangers, des laboratoires publics ou privés.



One-Pot Cascade Syntheses of Microporous and Mesoporous Pyrazine-Linked Covalent Organic Frameworks as Lewis-Acid Catalysts

Yunchao Ma,^{a,†} Xiaozhou Liu,^{a,†} Xinyu Guan,^a Hui Li,^a Yusran Yusran,^a Ming Xue,^a Qianrong Fang,^{a,*} Yushan Yan,^b Shilun Qiu^a and Valentin Valtchev^{a,c,*}

Covalent organic frameworks (COFs) are crystalline porous solids with broad potential applications. So far, the successful construction of COFs was limited to a few condensation reactions, and nearly all COFs were obtained by single-step synthesis based on predesigned linkers. Here, we report a general strategy in view of a one-pot cascade reaction to prepare both microporous and mesoporous fully π -conjugated pyrazine-linked COF materials (PZ-COFs). The obtained PZ-COFs show high chemical stability, large specific surface areas as well as H₂, CH₄ and CO₂ uptake capacities. Furthermore, we demonstrate that manganese(II)-incorporated PZ-COFs can act as excellent Lewis-acid catalysts for the cyanosilylation of aromatic aldehydes. This study not only provides a facile method to synthesize COFs required for multistep reactions but also expands the applications of COFs as promising catalysts.

Introduction

As a new class of crystalline porous polymers, covalent organic frameworks (COFs)^[1] have attracted considerable attention due to their outstanding potential in gas adsorption and separation,^[2] proton conduction,^[3] optoelectronics,^[4] drug deliver,^[5] chemical sensing,^[6] and especially heterogenous catalysis.^[7] Since the pioneering work of Yaghi in 2005,^[1a] a variety of two-dimensional (2D) COFs^[8] with eclipsed or staggered structures and three-dimensional (3D) COFs with the **ctn**,^[9] **bor**,^[10] **dia**^[11] or **pts**^[12] topology have been prepared over the past decade. However, owing to the complex nature of reversible synthesis, successful methods for the constructions of COF materials have been limited to a few chemical reactions, including three most commonly used types: boronic acid trimerization, boronate ester formation, and Schiff base reaction.^[1c,1d] Furthermore, nearly all COFs reported were obtained by single-step reaction based on predesigned linkers. As we all known, to obtain pure predesigned linkers is general difficulty, and thus the

exploration of new synthetic strategies, for example, obtaining linkers at the same time in synthesis of COFs, is an important and crucial task for the development of this promising class of porous materials.

Herein we report a new synthetic approach based on a one-pot cascade reaction strategy to produce COF materials. In view of this synthetic method, two microporous and mesoporous pyrazine-linked COFs, denoted PZ-COF-1 and PZ-COF-2, were successfully obtained by one-pot synthesis involving a two-step dehydration-oxidation reaction. Both materials show high chemical stability, impressive specific surface area, and promising gas storage capacities for H₂, CH₄ and CO₂. Furthermore, we demonstrate that PZ-COFs can incorporate manganese(II) ions by coordinating to nitrogen atoms of adjacent layers in PZ-COFs, and the resulting Mn(II)-assembled COF materials can act as excellent Lewis-acid catalysts for the cyanosilylation of aldehyde compounds.

Results and discussion

Our strategy for preparing PZ-COFs involves a one-pot dehydration and oxidation cascade reaction. As shown in Scheme 1a and 1b, 9,10-diazaanthracene (DAA) can be normally produced by the two-step path of the combination of both dehydration and oxidation reaction, which is a complicated process.^[13] Thus, we design the dehydration and oxidation cascade reaction to obtain DAA by one-pot synthesis of 1,2-diaminobenzene (DAB) and 1,2-dihydroxybenzene (DHB, Scheme 1c and Figure S1 in SI). On the basis of the same strategy, DHB is replaced by a flat triangular linker, hexahydroxy triphenylene (HHTP) and the DAB is substituted

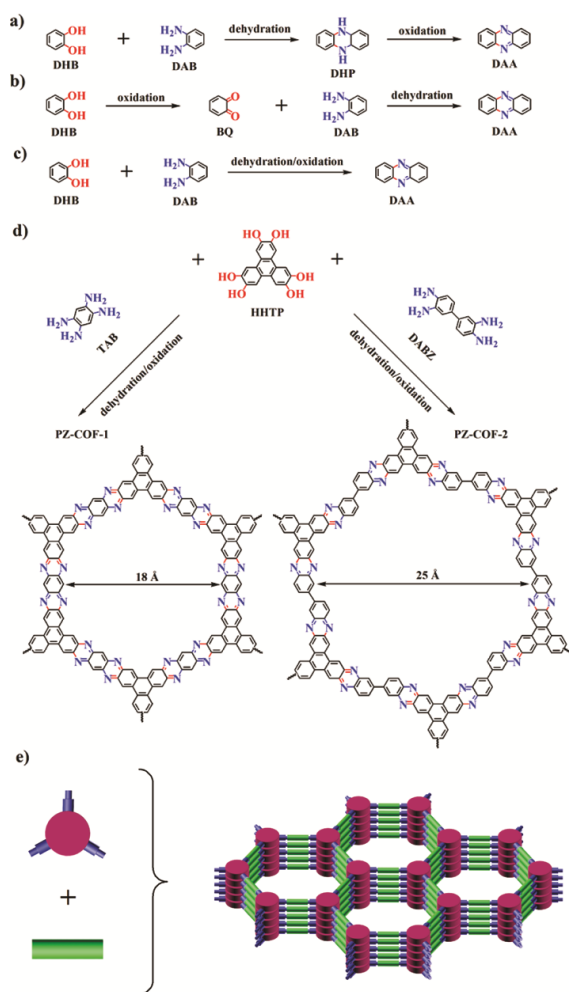
^a State Key Laboratory of Inorganic Synthesis and Preparative Chemistry, Jilin University, Changchun 130012, China. E-mail: qrfang@jlu.edu.cn

^b Department of Chemical and Biomolecular Engineering, Center for Catalytic Science and Technology, University of Delaware, Newark, DE 19716, USA

^c Normandie Univ, ENSICAEN, UNICAEN, CNRS, Laboratoire Catalyse et Spectrochimie, 6 Marechal Juin, 14050 Caen, France. E-mail: valentin.valtchev@ensicaen.fr

[†] These authors contributed equally to this work.

[‡] Electronic Supplementary Information (ESI) available: Procedure for the preparation of the COFs, TEM images, IR spectra, solid-state ¹³C NMR, TGA traces, PXRD patterns and simulations, BET plots, H₂, CO₂ and CH₄ adsorption-desorption isotherms, and fractional atomic coordinates. See DOI: 10.1039/x0xx00000x



Scheme 1 Strategy for preparing pyrazine-linked COFs (PZ-COFs).

(a) Two-step synthesis of DAA involving the dehydration of 1,2-diaminobenzene (DAB) and 1,2-dihydroxybenzene (DHB) followed by 5,10-dihydrophenazine (DHP) by the oxidation. (b) Two-step synthesis of DAA involving the oxidation of DHB followed by the dehydration of 1,2-benzoquinone (BQ) and DAB. (c) One-pot cascade dehydration and oxidation synthesis of DAA from DAB and DHB. (d) Expanded synthesis of hexahydroxy triphenylene (HHTP) and 1,2,4,5-tetraminobenzene (TAB) or 3,3'-diaminobenzidine (DABZ) to give 2D crystalline pyrazine-linked COFs, microporous PZ-COF-1 and mesoporous PZ-COF-2. (e) On the basis of triangular and linear building units, PZ-COFs show 2D hexagonal frameworks based on the boron nitride net (**bnn**).

by linkers with four amine groups, 1,2,4,5-tetraminobenzene (TAB) or 3,3'-diaminobenzidine (DABZ), yielding two new large-pore structures. These new COFs, denoted PZ-COF-1 and PZ-COF-2 exhibit pore diameter of 18 Å and 25 Å, respectively (Scheme 1d). In this case, HHTP can be defined as a 3-connected node, and TAB or DABZ can act as a 2-connected node, which results in 2D structures with the boron nitride net (**bnn**, Scheme 1e).^[14]

The syntheses of PZ-COFs were carried out by solvothermal reaction of HHTP, $K_2Cr_2O_7$ and TAB or DABZ in a mixed solution of *N*-methyl-2-pyrrolidone (NMP), mesitylene and acetic acid (AcOH), followed by heating at 120 °C for 3 days. The AcOH is employed as a catalyst to promote the dehydration reaction and $K_2Cr_2O_7$ is an oxidizer for the oxidation reaction. The conversion of the reactants was 85% for PZ-COF-1 and 83% for PZ-COF-2. The products, black solids, were insoluble in common organic solvents such as tetrahydrofuran (THF), acetone, methanol (MeOH), dichloromethane (CH_2Cl_2), chloroform ($CHCl_3$), hexane, *N,N*-dimethylformamide (DMF), dimethylsulfoxide (DMSO) and dioxane.

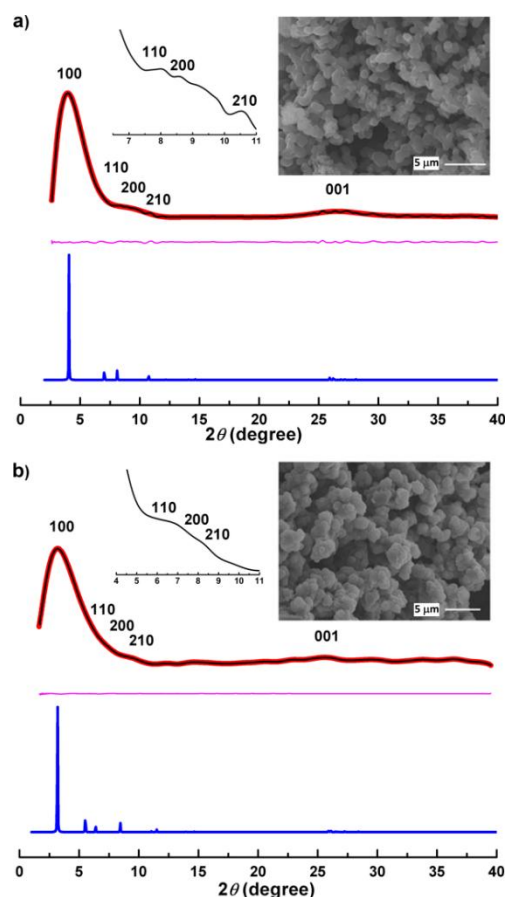


Fig. 1 PXRD patterns of PZ-COF-1 (a) and PZ-COF-2 (b) with the observed profile in black, refined in red, the difference (observed minus refined) in pink, and calculated based on the eclipsed structure in blue. Inset: enlarged experimental PXRD patterns and SEM images.

Scanning electron microscopy (SEM) and transmission electron microscopy (TEM) studies revealed that both PZ-COFs exhibited isometric morphology (Figure 1 inset, Figures S2 and S3 in SI). The particle size is about 1 μm for both materials; namely individual particles are observed in PZ-COF-1 while PZ-COF-2 contains complex aggregates. Fourier transform infrared (FT-IR) spectra of PZ-COFs (Figures S4-S8 in SI) showed the disappearance of the hydroxyl stretching band (3420 cm^{-1} for

HHTP), and the N-H stretching band (around 2952 cm^{-1} for TAB and 3388 cm^{-1} for DAB), indicating a completed conversion of these groups. Meanwhile, the characteristic stretching bands of pyrazine linkages (1256 and 1448 cm^{-1} for PZ-COF-1 as well as 1265 and 1448 cm^{-1} for PZ-COF-2) emerged in the IR spectra.^[8] The atomic order of PZ-COFs was further studied by solid-state ^{13}C cross-polarization magic-angle-spinning (CP/MAS) NMR spectroscopy (Figures S9 and S10 in SI). The two signals at $\delta = 125$ and 134 ppm for PZ-COF-1 and at $\delta = 124$ and 133 ppm for PZ-COF-2 can be assigned to different aromatic carbons, respectively. According to the thermogravimetric analysis (TGA), the PZ-COFs are stable up to about $300\text{ }^\circ\text{C}$ (Figure S11 in SI). We also tested the chemical stability of PZ-COFs by dispersing the samples in aqueous HCl (1 M) or NaOH (1 M) solutions and found that there was no change in their powder X-ray diffraction (PXRD) patterns (Figures S12 and S13 in SI).

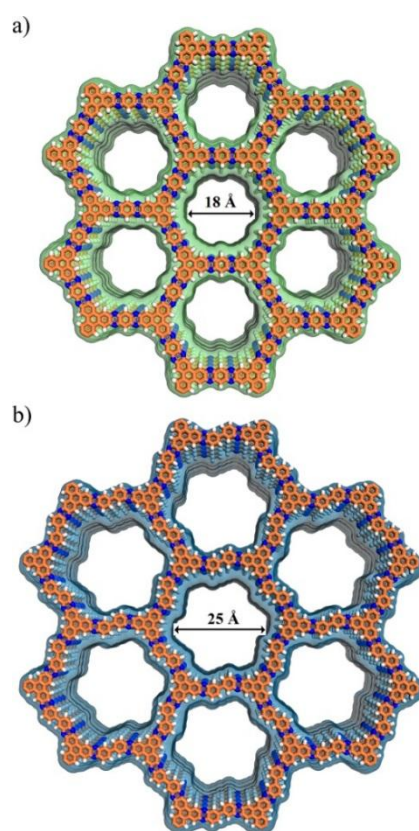


Fig. 2 Structural representations of microporous PZ-COF-1 (a) and mesoporous PZ-COF-2 (b). C, yellow; N, blue; H, white.

The crystalline nature of new PZ-COFs was confirmed by PXRD analysis (Figure 1). After a geometrical energy minimization by using the Materials Studio Software package^[15] based on the eclipsed structure the unit cell parameters were determined. PZ-COF-1 exhibits space group $P6_3/mmm$ (No. 191) with unit cell of $a = b = 25.184\text{ }^\circ\text{Å}$, $c = 3.439\text{ }^\circ\text{Å}$, $\alpha = \beta = 90^\circ$, and $\gamma = 120^\circ$. PZ-COF-2 shows space group $P6_3/m$ (No. 175) with unit cell of $a = b = 32.009\text{ }^\circ\text{Å}$, $c = 3.440\text{ }^\circ\text{Å}$, $\alpha = \beta =$

90° , and $\gamma = 120^\circ$. Simulated PXRD patterns show good match with the experimental ones (Figure 1, black and blue curves). In addition, the full profile pattern matching (Pawley) refinements are performed from the experimental PXRD patterns. PXRD peaks at 4.05 , 7.01 , 8.10 , 10.72 and 25.87° for PZ-COF-1 can be assigned to the (100), (110), (200), (210) and (001) Bragg peaks. The peaks at 3.18 , 5.53 , 6.39 , 8.45 and 25.89° for PZ-COF-2 correspond to the (100), (110), (200), (210) and (001) Bragg peaks, respectively. The refinement results revealed unit cell parameters nearly equivalent to the predictions with excellent agreement factors ($a = b = 25.761\text{ }^\circ\text{Å}$, $c = 3.555\text{ }^\circ\text{Å}$, $\alpha = \beta = 90^\circ$, $\gamma = 120^\circ$, $wR_p = 1.72\%$, and $R_p = 0.69\%$ for PZ-COF-1; $a = b = 32.521\text{ }^\circ\text{Å}$, $c = 3.532\text{ }^\circ\text{Å}$, $\alpha = \beta = 90^\circ$, $\gamma = 120^\circ$, $wR_p = 1.91\%$, and $R_p = 0.89\%$ for PZ-COF-2). Besides the eclipsed structure, we also considered an alternative staggered model, which was set up from the space groups of $P6_3/mmc$ (No. 194) for PZ-COF-1 or $P6_3/m$ (No. 176) for PZ-COF-2. However, these calculated patterns did not match the experimental PXRD patterns (Figures S14-19 and Tables S1-4 in SI). On the basis of the above results, we can state that both PZ-COFs have the expected architectures with the eclipsed model, which show the microporous hexagonal pores with diameter of about $18\text{ }^\circ\text{Å}$ for PZ-COF-1 and mesoporous channels with diameter of about $25\text{ }^\circ\text{Å}$ for PZ-COF-2 (Figure 2).

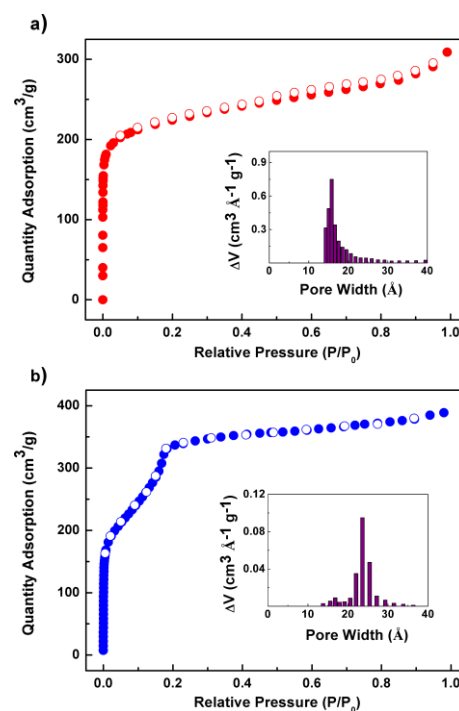
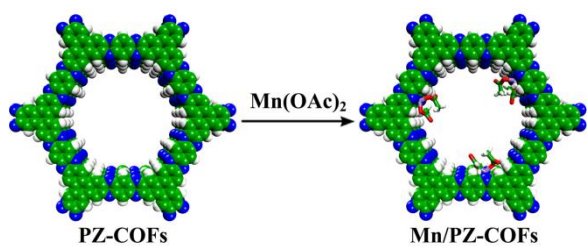


Fig. 3 N_2 adsorption-desorption isotherms of microporous PZ-COF-1 (a) and mesoporous PZ-COF-2 (b) at 77 K . Inset: the pore size distribution.

The specific surface area and porosity of PZ-COFs were determined by measuring N_2 adsorption at 77 K . As can be seen in Figure 3, PZ-COF-1 exhibited the characteristic for

microporous materials type I isotherm with sharp uptake below 0.05 P/P_0 . Type IV isotherm with a two-steepest uptake below 0.2 P/P_0 , which is typical of ordered mesoporous materials, was recorded for PZ-COF-2. The absence of hysteresis during desorption for PZ-COF-2 is a common feature of materials containing hexagonally aligned 1D mesopores.^[16] The application of the Brunauer-Emmett-Teller (BET) model in the low pressure region ($0.005 < P/P_0 < 0.105$) showed a BET surface areas of $845 \text{ m}^2 \text{ g}^{-1}$ for PZ-COF-1 and $1130 \text{ m}^2 \text{ g}^{-1}$ for PZ-COF-2 (Figures S20 and S21 in SI). The pore-size distributions of PZ-COFs were calculated by nonlocal density functional theory (NLDFT) and showed a narrow pore width (16 \AA for PZ-COF-1 and 24 \AA for PZ-COF-2, Figure 3 inset), which was in good agreement with the pore sizes predicted from their crystal structures (18 \AA for PZ-COF-1 and 25 \AA for PZ-COF-2). In addition the adsorption of H_2 , CO_2 and CH_4 for both PZ-COFs was studied in order to evaluate their potential application in gas storage (Figures S22-24 in SI). PZ-COF-1 showed uptake of $121 \text{ cm}^3 \text{ g}^{-1}$ of H_2 , $68 \text{ cm}^3 \text{ g}^{-1}$ of CO_2 and $14 \text{ cm}^3 \text{ g}^{-1}$ of CH_4 . The mesoporous PZ-COF-2 could store up to $156 \text{ cm}^3 \text{ g}^{-1}$ of H_2 , $91 \text{ cm}^3 \text{ g}^{-1}$ of CO_2 and $21 \text{ cm}^3 \text{ g}^{-1}$ of CH_4 .



Scheme 2 Schematic representation for the syntheses of Mn/PZ-COFs.

Encouraged by high porosity and the appropriate distance ($\sim 3.4 \text{ \AA}$) of eclipsed nitrogen atoms in adjacent layers, which makes PZ-COFs an ideal scaffold for incorporating metal ions,^[7a] we successfully assembled the manganese(II)-coordinated COF materials (denoted as Mn/PZ-COFs), and explored their catalytic potential for the cyanosilylation of aldehyde compounds. Typically, through a simple post-treatment of PZ-COFs with manganese acetate, $\text{Mn}(\text{OAc})_2$, Mn/PZ-COFs were readily prepared (Scheme 2 and see SI for details). A comparison of PXRD patterns of PZ-COFs and Mn/PZ-COFs revealed that crystal structures of PZ-COFs were well preserved after the treatment with $\text{Mn}(\text{OAc})_2$ (Figures S25 and S26 in SI). SEM images suggested that layer structures of PZ-COFs also remained unchanged after the reaction with $\text{Mn}(\text{OAc})_2$ (Figures S27 and S28 in SI). The well-dispersed manganese species could be clearly observed in the energy dispersive X-ray (EDX) mapping analysis (Figures S29 and S30 in SI). Nitrogen adsorption isotherms at 77 K of Mn/PZ-COFs indicated a lower N_2 adsorption which is due to the presence of $\text{Mn}(\text{OAc})_2$ in the pores (Figures S31 and S32 in SI). Manganese content of 6.3 wt% for Mn/PZ-COF-1 and 6.6 wt% for Mn/PZ-COF-2 was determined by ICP analysis. X-ray

photoelectron spectroscopy (XPS, Figure S33 in SI) showed that the binding energies of Mn $2p_{3/2}$ in Mn/PZ-COFs were about 642 eV, indicating that the Mn species were in +2 state. Mn/PZ-COFs and a model complex Mn/Phen (Phen = 1,10-phenanthroline) had a similar shift of 1 eV in comparison with that of free $\text{Mn}(\text{OAc})_2$, which suggested that Mn ions were most probably located in between the adjacent layers of PZ-COFs and efficiently coordinated with two nitrogen atoms from different layers.^[7a]

Table 1 Catalytic activities of Mn/PZ-COFs in the cyanosilylation of aldehyde compounds^a

Entry	Ar	Catalyst	Time (h)	Yield (%) ^b
1	phenyl	Mn/PZ-COF-1	6	98
2	phenyl	Mn/PZ-COF-2	5	99
3	biphenyl	Mn/PZ-COF-1	6	97
4	biphenyl	Mn/PZ-COF-2	5	97
5	1-naphthyl	Mn/PZ-COF-1	6	96
6	1-naphthyl	Mn/PZ-COF-2	5	97
7	methoxyphenyl	Mn/PZ-COF-1	8	97
8	methoxyphenyl	Mn/PZ-COF-2	8	98
9	nitrophenyl	Mn/PZ-COF-1	3	96
10	nitrophenyl	Mn/PZ-COF-2	3	98

^a Reaction conditions: Me_3SiCN (1.0 mmol), aldehyde (1.0 mmol), dry CH_2Cl_2 (6.0 mL), Mn/PZ-COF-1 or Mn/PZ-COF-2 (0.1 mmol), room temperature, under Ar. ^b Determined by ^1H NMR based on the starting materials.

The catalytic activities of Mn/PZ-COFs were subsequently examined in one of the representative Mn(II)-catalyzed reactions, i.e., the cyanosilylation reaction, which is an important step to key derivatives in the syntheses of fine chemicals and pharmaceuticals.^[17] The catalytic reactions were performed with 1.0 mmol of each reactant in dry CH_2Cl_2 (6.0 mL) with PZ-COF-1 or PZ-COF-2 (10 mol%) at room temperature for 5~6 h. The conversion and the product distribution were monitored by ^1H NMR spectroscopy based on the starting materials. As shown in Table 1, Me_3SiCN reacted with benzaldehyde to form the product α -(trimethylsilyloxy)phenylacetonitrile (Ar = phenyl) in excellent yields (98% for Mn/PZ-COF-1 and 99% for Mn/PZ-COF-2). Furthermore, by replacing benzaldehyde reactant with 4-biphenylcarboxaldehyde, 1-naphthaldehyde, 4-methoxybenzaldehyde or 4-nitrobenzaldehyde, and keeping all other conditions the same, high yields (96-99%) can be obtained under different reaction time (3-8 hrs, Table 1). Figures 4, S34 and S35 depict the concentration of products as a function of time. We verified that the reaction was indeed catalyzed by Mn/PZ-COFs instead of free $\text{Mn}(\text{OAc})_2$ by a control experiment, in which the catalyst was removed from the reaction mixture after 1 h, and the isolated solution was

retained under the same reaction conditions. No further conversion was observed in this case (Figure S36 in SI). After the catalytic reactions, the results of PXRD confirmed the structural integrity of Mn/PZ-COFs, thus revealing the high stability of new COF materials in the cyanosilylation reaction (Figures S37 and S38 in SI). The COF crystals can be easily isolated from the reaction mixture by a simple filtration and reused at least four times with almost no loss of activity and similar TOF (Figures S39 and S40 in SI).

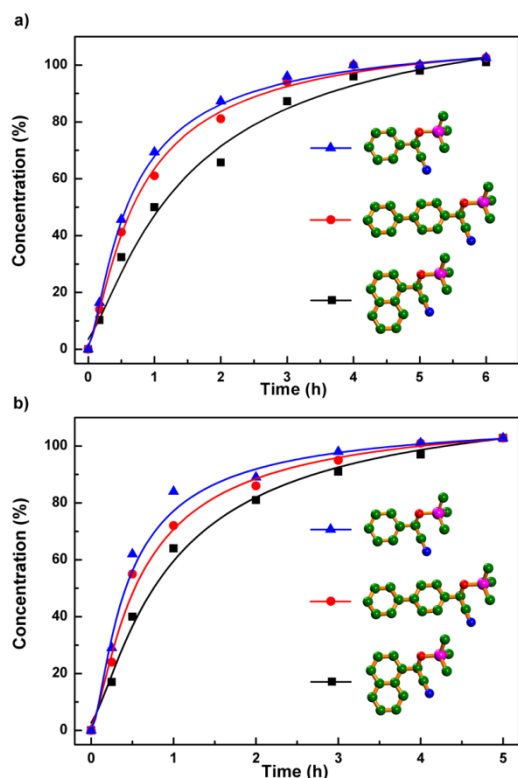


Fig. 4 Concentration (%) versus time (h) for the cyanosilylation of benzaldehyde (blue), 4-biphenylcarboxaldehyde (red), and 1-naphthaldehyde (black) on Mn/PZ-COF-1 (a) and Mn/PZ-COF-2 (b). Inset: the structures of products. C, green; N, blue; O, red; Si, pink. H atoms are not shown for clarity.

Conclusions

In conclusion, we have developed a new synthetic strategy to construct COF materials by employing one-pot dehydration and oxidation cascade reactions. Two novel 2D COFs, microporous PZ-COF-1 and mesoporous PZ-COF-2, were prepared. These new materials showed high chemical stability, large specific surface areas as well as promising H_2 , CH_4 and CO_2 uptake capacities. In addition, we explored the incorporation of Mn(II) in PZ-COFs and found that manganese-coordinated COFs can act as excellent Lewis-acid catalysts. One-pot cascade synthesis for COF materials exemplified in this work may not only expand the development of COFs with innovative synthesis strategy, but also promote the applications of functional COFs.

Acknowledgements

This work was supported by National Natural Science Foundation of China (21571079, 21621001, 21390394, 21571076, and 21571078), “111” project (B07016 and B17020), Guangdong Science and Technology Department Project (2012D0501990028), and the program for JLU Science and Technology Innovative Research Team. Q.F. and V.V. acknowledge the support from Thousand Talents program (China). V.V., Q.F. and S.Q. acknowledge the collaboration in the framework of China-French joint laboratory “Zeolites”.

Notes and references

- (a) A. P. Côté, A. I. Benin, N. W. Ockwig, M. O’Keeffe, A. J. Matzger, O. M. Yaghi, *Science*, **2005**, *310*, 1166; (b) J. W. Colson, A. R. Woll, A. Mukherjee, M. P. Levendorf, E. L. Spitler, V. B. Shields, M. G. Spencer, J. Park, W. R. Dichtel, *Science*, **2011**, *332*, 228; (c) X. Feng, X. S. Ding, D. L. Jiang, *Chem. Soc. Rev.*, **2012**, *41*, 6010; (d) S. Y. Ding, W. Wang, *Chem. Soc. Rev.*, **2013**, *42*, 548. (e) C. S. Diercks, O. M. Yaghi, *Science*, **2017**, *355*, 923.
- (a) H. Furukawa, O. M. Yaghi, *J. Am. Chem. Soc.*, **2009**, *131*, 8875; (b) S. S. Han, J. L. Mendoza-Cortes, W. A. Goddard, *Chem. Soc. Rev.*, **2009**, *38*, 1460; (c) X. Y. Guan, Y. C. Ma, H. Li, Y. Yusran, M. Xue, Q. R. Fang, Y. S. Yan, V. Valtchev, S. L. Qiu, *J. Am. Chem. Soc.*, **2018**, *140*, 4494.
- (a) S. Chandra, T. Kundu, S. Kandambeth, R. BabaRao, M. Y. arathe, S. M. Kunjir, R. Banerjee, *J. Am. Chem. Soc.*, **2014**, *136*, 6570; (b) H. Xu, S. S. Tao, D. L. Jiang, *Nat. Mater.*, **2016**, *15*, 722; (c) H. P. Ma, B. L. Liu, B. Li, L. M. Zhang, Y. G. Li, H. Q. Tan, H. Y. Zang, G. S. Zhu, *J. Am. Chem. Soc.*, **2016**, *138*, 5897.
- (a) S. Wan, J. Guo, J. Kim, H. Ihee, D. Jiang, *Angew. Chem. Int. Ed.*, **2008**, *47*, 8826; (b) G. H. V. Bertrand, V. K. Michaelis, T. C. Ong, R. G. Griffin, M. Dinca, *Proc. Natl. Acad. Sci. USA*, **2013**, *110*, 4923; (c) M. Dogru, T. Bein, *Chem. Commun.*, **2014**, *50*, 5531; (d) X. H. Liu, C. Z. Guan, D. Wang, L. J. Wan, *Adv. Mater.*, **2014**, *26*, 6912.
- (a) Q. R. Fang, J. H. Wang, S. Gu, R. B. Kaspar, Z. B. Zhuang, J. Zheng, H. X. Guo, S. L. Qiu, Y. S. Yan, *J. Am. Chem. Soc.*, **2015**, *137*, 8352; (b) L. Y. Bai, S. Z. F. Phua, W. Q. Lim, A. Jana, Z. Luo, H. P. Tham, L. Z. Zhao, Q. Gao, Y. L. Zhao *Chem. Commun.*, **2016**, *52*, 4128.
- (a) Q. R. Fang, Z. B. Zhuang, S. Gu, R. B. Kaspar, J. Zheng, J. H. Wang, S. L. Qiu, Y. S. Yan, *Nat. Commun.*, **2014**, *5*, 4503; (b) G. Das, B. P. Biswal, S. Kandambeth, V. Venkatesh, G. Kaur, M. Addicoat, T. Heine, S. Verma, R. Banerjee, *Chem. Sci.*, **2015**, *6*, 3931.
- (a) S. Y. Ding, J. Gao, Q. Wang, Y. Zhang, W. G. Song, C. Y. Su, W. Wang, *J. Am. Chem. Soc.*, **2011**, *133*, 19816; (b) Q. R. Fang, S. Gu, J. Zheng, Z. B. Zhuang, S. L. Qiu, Y. S. Yan, *Angew. Chem., Int. Ed.*, **2014**, *53*, 2878; (c) X. R. Wang, X. Han, J. Zhang, X. W. Wu, Y. Liu, Y. Cui, *J. Am. Chem. Soc.*, **2016**, *138*, 12332; (d) C. S. Diercks, S. Lin, N. Kornienko, E. A. Kapustin, E. M. Nichols, C. H. Zhu, Y. B. Zhao, C. J. Chang, O. M. Yaghi, *J. Am. Chem. Soc.*, **2018**, *140*, 1116; (e) Y. P. Song, Q. Sun, B. Aguila, S. Q. Ma, *Adv. Sci.*, **2018**, 1801410; (f) J. Zhang, X. Han, X. W. Wu, Y. Liu, Y. Cui, *J. Am. Chem. Soc.*, **2017**, *139*, 8277; (g) X. Han, Q. C. Xia, J. J. Huang, Y. Liu, C. X. Tan, Y. Cui, *J. Am. Chem. Soc.*, **2017**, *139*, 8693; (h) Q. Sun, B. Aguila, J. Perman, N. Nguyen, S. Q. Ma, *J. Am. Chem. Soc.*, **2016**, *138*, 15790; (i) S. Lin, C. S. Diercks, Y. B. Zhang, N. Kornienko, E. M. Nichols, Y. B. Zhao, A. R. Paris, D. Kim, P. D. Yang, O. M. Yaghi, C. J. Chang, *Science*, **2015**, *349*, 1208.
- (a) J. W. Colson, W. R. Dichtel, *Nat. Chem.*, **2013**, *5*, 453; (b) Y. L. Zhu, S. Wan, Y. H. Jin, W. Zhang, *J. Am. Chem. Soc.*,

- 2015, 137, 13772; (c) Y. F. Zeng, R. Y. Zou, Z. Luo, H. C. Zhang, X. Yao, X. Ma, R. Q. Zou, Y. L. Zhao, *J. Am. Chem. Soc.*, **2015**, 137, 1020; (d) X. Chen, M. Addicoat, E. Q. Jin, H. Xu, T. Hayashi, F. Xu, N. Huang, S. Irle, D. L. Jiang, *Sci. Rep.*, **2015**, 5, 14650; (e) Y. Du, H. S. Yang, J. M. Whiteley, S. Wan, Y. H. Jin, S. H. Lee, W. Zhang, *Angew. Chem. Int. Ed.*, **2016**, 55, 1737; (f) J. W. Crowe, L. A. Baldwin, P. L. McGrier, *J. Am. Chem. Soc.*, **2016**, 138, 10120; (g) L. Ascherl, T. Sick, J. T. Margraf, S. H. Lapidus, M. Calik, C. Hettstedt, K. Karaghiosoff, M. Döblinger, T. Clark, K. W. Chapman, F. Auras, T. Bein, *Nat. Chem.*, **2016**, 8, 310; (h) P. Kuhn, M. Antonietti, A. Thomas, *Angew. Chem. Int. Ed.*, **2008**, 47, 3450; (i) J. Guo, Y. H. Xu, S. B. Jin, L. Chen, T. Kaji, H. Ono, Addicoat, M. A.; Kim, J.; Saeki, A.; Ihee, H.; Seki, S.; Y. Irle, S.; M. Hiramoto, J. Gao, D. L. Jiang, *Nat. Commun.*, **2013**, 4, 2736.
- 9 (a) H. M. El-Kaderi, J. R. Hunt, J. L. Mendoza-Cortes, A. P. Côté, R. E. Taylor, M. O'Keeffe, O. M. Yaghi, *Science*, **2007**, 316, 268; (b) H. Li, Q. Y. Pan, Y. C. Ma, X. Y. Guan, M. Xue, Q. R. Fang, Y. S. Yan, V. Valtchev, S. L. Qiu, *J. Am. Chem. Soc.*, **2016**, 138, 14783.
- 10 L. A. Baldwin, J. W. Crowe, P. D. A. yles, P. L. McGrier, *J. Am. Chem. Soc.*, **2016**, 138, 15134.
- 11 (a) F. J. Uribe-Romo, J. R. Hunt, H. Furukawa, C. Klöck, M. O'Keeffe, O. M. Yaghi, *J. Am. Chem. Soc.*, **2009**, 131, 4570; (b) D. Beaudoin, T. Maris, J. D. Wuest, *Nat. Chem.*, **2013**, 5, 830; (c) Y. B. Zhang, J. Su, H. Furukawa, Y. F. Yun, F. Gandara, A. Duong, X. D. Zou, O. M. Yaghi, *J. Am. Chem. Soc.*, **2013**, 135, 16336.
- 12 G. Q. Lin, H. M. Ding, D. Q. Yuan, B. S. Wang, C. Wang, *J. Am. Chem. Soc.*, **2016**, 138, 3302.
- 13 J. S. Morley, *J. Chem. Soc.*, **1952**, 4008.
- 14 A. P. Côté, H. M. El-Kaderi, H. Furukawa, J. R. Hunt, O. M. Yaghi, *J. Am. Chem. Soc.*, **2007**, 129, 12914.
- 15 *Materials Studio ver. 7.0*; Accelrys Inc.; San Diego, CA.
- 16 M. Thommes, in *Nanoporous Materials Science and Engineering* (Imperial College Press, 2004).
- 17 (a) K. Higuchi, M. Onaka, Y. Izumi, *Bull. Chem. Soc. Jpn.*, **1993**, 66, 2016; (b) R. J. H. Gregory, *Chem. Rev.*, **1999**, 99, 3649.